Available online at www.sciencedirect.com
SCIENCE DIRECT
Thermochimica Acta 438 (2005) 134–143
thermochimica acta
www.elsevier.com/locate/tca

Tantalum and niobium perovskite oxynitrides: Synthesis and analysis of the thermal behaviour

A. Rachel [a], S.G. Ebbinghaus [a,*], M. Güngerich [b], P.J. Klar [b], J. Hanss [a], A. Weidenkaff [c], A. Reller [a]

[a] *Lehrstuhl für Festkörperchemie, Institut für Physik, Universität Augsburg, Universitätsstraße 1, D-86159 Augsburg, Germany*
[b] *Fachbereich Physik und WZMW, Renthof 5, D-35032 Marburg, Germany*
[c] *Festkörperchemie und Analytik, EMPA, Ueberlandstrasse 129, CH-8600 Duebendorf, Switzerland*

Received 18 May 2005; received in revised form 25 July 2005; accepted 3 August 2005
Available online 30 September 2005

Abstract

Ta^{5+} and Nb^{5+}-based oxynitride perovskites of the ABO_2N type (A = Ca, Sr, Ba) were synthesised by ammonolysis of complex oxide precursors. These precursors were either crystalline perovskites or amorphous xerogels prepared by solid–solid reaction and by soft chemistry methods, respectively. Phase purity of the oxynitrides was verified by X-ray diffraction (XRD) and their crystal structures were determined by Rietveld refinements. The morphology of the obtained powders was characterised by scanning electron microscopy (SEM). Thermal stability was investigated by thermogravimetric analysis (TGA) coupled with mass spectroscopy. Oxidation studies reveal an intermediate product that gives rise to a characteristic weight gain in the TG curve. This intermediate was found for all the examined oxynitrides in oxidising atmosphere. Investigations by Raman scattering revealed the presence of dinitrogen (N≡N) loosely bound to B and N≡B bonds (B = transition metal) in the intermediate compounds. Mass spectral analysis confirmed molecular nitrogen evolution indicating that N_2 is retained during the oxidation reaction. At higher temperatures (T = 800–1000 °C) the dinitrogen is released leading to the formation of the corresponding oxides.

Keywords: Oxynitride perovskites; XRD Rietveld refinements; Ammonolysis; Thermal oxidation; Raman spectroscopy

1. Introduction

There is an ongoing quest for new materials possessing improved properties especially in electronics, energy conversion and environmental applications. Perovskite-type compounds are of particular interest since it is possible to control the properties of these materials by suitably modifying their composition. This leads to changes in their crystallographic and electronic structures. While cation substitutions have been investigated since decades [1], comparatively little is known about anion-substituted perovskites, especially about oxynitrides [2]. However, transition metal oxynitrides are interesting for various possible applications [3] because of their unusual dielectric behaviour [4], transport [5] and optical properties [6], ionic conductivity [7] as well as their catalytic activity. For instance they are able to act as substitutes for noble metal catalysts like Ir, Pt and Pd [8]. Currently, the photocatalytic reactivity for the photolysis of water has been studied [9]. Their refractive index and colour also suggest novel opto-electronic applications [10,11]. Additionally, perovskite oxynitrides have been suggested as non-toxic and eco-friendly potential substitutes for toxic metals in the yellow–orange–red Cd(S,Se) pigments [12,13].

Oxynitride perovskites are generally derived from the corresponding oxides by introducing nitrogen into the anionic network. The resulting increase of negative charge is compensated by (i) cationic substitution at the A site (e.g. $La_{2/3}Ta_2O_6 \rightarrow A_xLa_{2/3}Ta_2O_{6-x}N_x$ where A = Na, Li [7]), (ii) changes in the oxidation state of the transition metal (e.g.

* Corresponding author. Tel.: +49 821 598 3012; fax: +49 821 598 3002.
E-mail address: stefan.ebbinghaus@physik.uni-augsburg.de (S.G. Ebbinghaus).

0040-6031/$ – see front matter © 2005 Elsevier B.V. All rights reserved.
doi:10.1016/j.tca.2005.08.010

$SrMoO_4 \rightarrow SrMoO_{2.5}N_{0.5}$ [14]), and (iii) reduction of the number of anions (e.g. $CaTaO_{3.5} \rightarrow CaTaO_2N$ [15,16]).

The conventional synthesis for oxynitrides is by ammonolysis [15]. Other non-conventional synthesis routes are, e.g. reactions of TaON with alkaline earth oxides [17], plasma nitridation [18], thermal decomposition of ammonia adducts [19], or the use of azides as nitrogen source [20]. One disadvantage of the classical ammonolysis is that the reactions are usually slow, i.e. many reaction cycles have to be carried out to achieve pure oxynitrides. In many cases halides were used as mineralisers to increase the reaction rate [12,21,22]. On the other hand, it is well known that soft chemistry methods, especially the decomposition of citrate complexes lead to fine particles which in most cases possess a high reactivity [9,23]. In this paper we present the preparation of alkaline earth oxynitrides of Nb and Ta by both conventional solid state technique and ammonolysis of decomposed citrate precursors. The different samples are compared with respect to their morphology, physical properties and thermal stability.

2. Experimental

2.1. Synthesis procedure

Oxynitrides ABO_2N (A = Ca, Sr, B = Nb, Ta) were prepared from their oxide precursors $A_2B_2O_7$. The synthesis of the precursors was carried out by either soft-chemistry methods [24,25] or conventional solid–solid reactions. Since for the Ba compounds $A_2B_2O_7$ phases do not exist, the reactions lead to mixtures of $Ba_5B_4O_{15}$ and BaB_2O_6 with a corresponding nominal composition.

2.2. Ceramic synthesis

Stoichiometric amounts of the starting materials $CaCO_3$ (Merck), $SrCO_3$ (Aldrich), $BaCO_3$ (Aldrich), Ta_2O_5 (Serva), Nb_2O_5 (Aldrich) were mixed with iso-propanol and were well ground in an agate mortar. After drying, the powders were placed in alumina crucibles and heated at 1000 °C for 24 h (Ca-oxides) and 1100 °C for 48 h (Sr-oxides), respectively. For the Ba–Ta/Nb-oxides, a stepwise calcination from 1000 to 1150 °C for 24 h was carried out with intermediate grindings.

2.3. Soft-chemistry method

The synthesis procedure for the oxide/xerogel precursors using citric acid as the complexing agent is outlined in Fig. 1. Gels containing the corresponding metal cations were prepared by dissolving 0.01 M of $TaCl_5$ (Merck) or $NbCl_5$ (Riedel-de Haen) with 0.04 M anhydrous citric acid (Fluka) in dry ethanol. Stoichiometric amounts of aqueous solutions (0.01 M) of the corresponding metal nitrates $Ca(NO_3)_2{\cdot}4H_2O$ (Fluka), $Sr(NO_3)_2$ (Fluka), $Ba(NO_3)_2$ (Aldrich) were added. In case of tantalates the solutions in some cases turned turbid because of precipitated metal hydroxides. Therefore, these solutions were heated at 60 °C until re-dissolution of the hydroxides was achieved. Stirring was further continued for 12 h to obtain stable A-Ta/Nb-citrate complexes (A = Ca, Sr, Ba). Afterwards, the solvent was removed on a rotary evaporator. The solution became progressively viscous and when heated at 90 °C for 12 h, a bubbly gel was obtained. The product was oven dried for 12 h at 120 °C and for 24 h at 200 °C. The organic constituents were destroyed by burning the dried A-Ta/Nb-citrate gels at 650 °C, which resulted in purely white powders. These powders are denoted as xerogel precursors in the following.

To obtain crystalline $A_2B_2O_7$-type oxides, these amorphous xerogel precursors were calcined in air at 1000 °C for 24 h.

2.4. Ammonolysis

The oxide precursors (crystalline $A_2B_2O_7$ and amorphous xerogels, respectively) were treated with flowing ammonia to obtain the intended oxynitrides. To study the effect of halide-mineralisers, equimolar amounts of NaCl were added to some of the reaction mixtures. Roughly 1 g of each sample was weighed into an alumina boat and placed in the reaction quartz tube that was flushed with N_2 gas. The tube was evacuated and refilled with ammonia. Ammonolysis was carried out with an ammonia gas flow of 50–150 ml/min in the temperature range between 600 and 1000 °C. After 18 h the furnace was switched off and allowed to cool down. When the temperature was below 250 °C, the ammonia flow was changed to nitrogen. Thereafter, the samples were cooled to room temperature in nitrogen atmosphere. This procedure was repeated until single-phase oxynitrides were obtained.

2.5. Characterisation

The microstructure of the samples was specified with a Philips FEI XL 30 FEG Environmental Scanning Electron Microscope. X-ray patterns were measured with Cu Kα radiation using a Seifert XRD 3003-TT diffractometer. Data used for confirming phase purity were recorded in a 2θ regime of 10–80° (step scan of 0.020° with a counting time of 2 s per step). For the refinement of cell parameters, XRD patterns were collected in the range 15–150° 2θ (step width 0.010° with counting time 5 s per step).

The thermal degradation of the oxide precursors prepared by the citrate route and the thermal stability of oxynitrides in oxidising atmosphere were investigated on a NETZSCH STA 409C thermobalance connected to a Balzers QMG quadrupole mass spectrometer by a skimmer coupling system. For the decomposition of the citrate precursors the measurements were carried out in the range of 25–1200 °C in synthetic air with a heating rate of 10 K/min. The oxidation reactions of the oxynitrides were performed in an oxidising

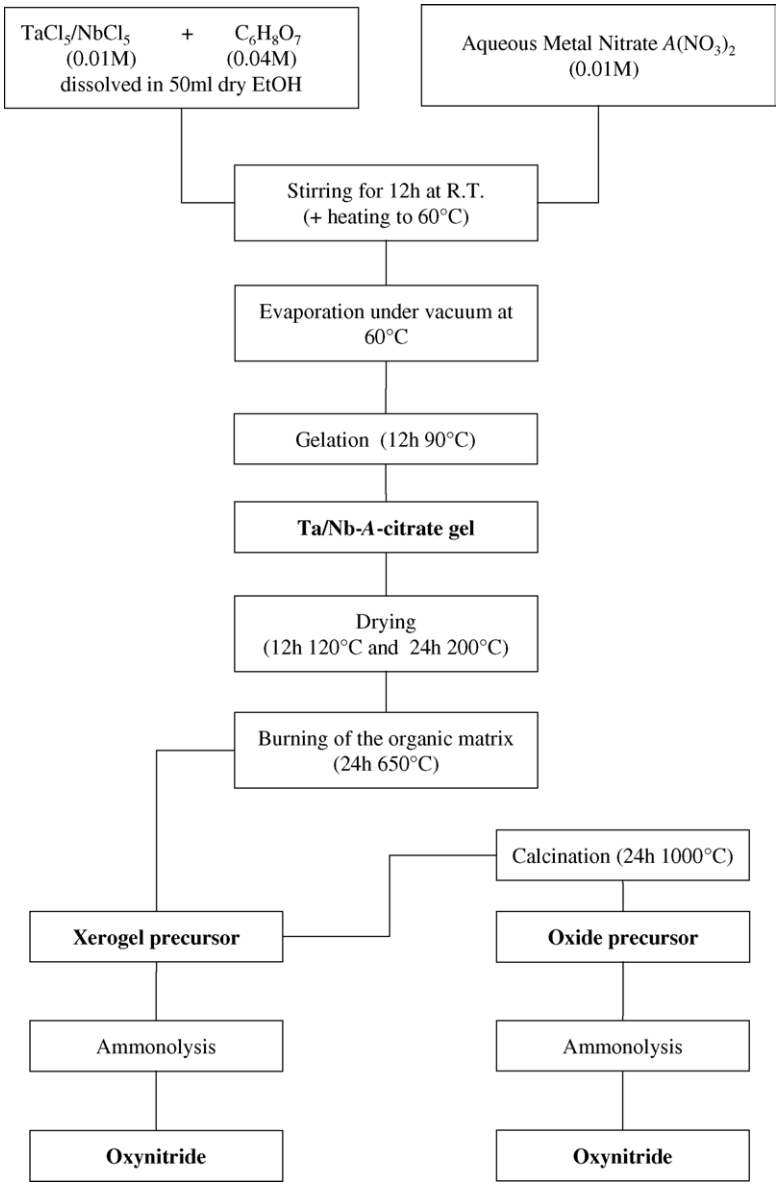

Fig. 1. Flow chart for the synthesis of oxynitrides by the soft chemistry method.

atmosphere of 80% Ar/20% O_2 and 99% Ar/1% O_2, respectively.

Raman scattering experiments were performed at room temperature in back-scattering geometry using a Jobin Yvon micro-Raman system based on an Olympus BX41 optical microscope. Circularly polarised excitation light (514.5 nm) of an Ar^+ laser (Coherent Innova 200) was coupled via optical fibres into the microscope system and focused onto the sample. The laser power on the sample was kept below 10 mW to avoid laser-induced chemical decomposition. The scattered light was collected via the microscope objective. Elastically scattered light was rejected by a Kaiser Optics holographic Notch filter before coupling the Raman scattered light into the spectrometer system (Acton Research corporation SpectraPro-500). The spectra were detected by a liquid nitrogen cooled ISA CCD2000 camera.

3. Results and discussion

3.1. Synthesis of oxide/xerogel precursors

In the following section the classical solid state reaction pathway is compared with the soft chemistry citrate route. The latter involves the complex formation of the different cations, the polymerisation of the complexing agent and finally the decomposition of the organic matrix resulting in the powder precursor. Citric acid was used as complexing agent because it has the advantage of forming stable solutions with varying stoichiometries. Hence, it can be used to synthesise a large number of compositions, which cannot be obtained by conventional solid state methods. It was found that temperature is an important factor during complexation, because insoluble precipitates, which were formed due to

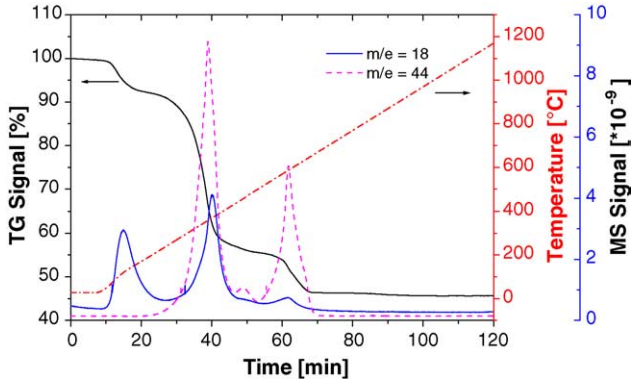

Fig. 2. TG curve of strontium niobium xerogel showing the decomposition of the citrate xerogel to the oxide precursor.

hydrolysis of $TaCl_5$ could be dissolved completely by moderate heating of the reaction mixture.

To establish an appropriate decomposition temperature for the organic matrix, oxidation of the different citrate gels was investigated by thermoanalytic measurements. As an example, Fig. 2 shows the reaction of a Sr–Nb-gel during heating from room temperature to 1200 °C. Volatile reaction products were monitored by mass spectroscopy. As can be seen the reaction involves three major steps. The first step occurs between approximately 100 and 150 °C and is accompanied by a loss of water ($m/e = 18$). It can therefore be assigned to a "drying" of the gel that might either be due to an evaporation of absorbed water or to a continuing polycondensation of the citric acid. The main weight loss occurs between 250 and 400 °C. Within this temperature range the vast majority of the organic matrix is burned as can be seen by the evolution of both H_2O and CO_2 ($m/e = 44$). Finally, a third weight loss is observed at about 600 °C. Again, mass spectroscopy shows the formation of CO_2 and small amounts of H_2O. This last step is either caused by the burning of the residual organic component or due to the decomposition of bicarbonates formed in the preceding step.

The formation of crystalline phases during decomposition of the precursors was analysed by ex-situ XRD. The X-ray profiles of the xerogel/oxide precursor calcined at different temperatures are shown in Figs. 3 and 4 for the strontium–niobium and strontium–tantalum xerogel precursors, respectively. The structural evolution of the oxide perovskite is revealed by the progressive crystallisation of the amorphous precursor starting at around 600 °C. At 1000 °C the XRD patterns correspond to the single-phase layered perovskite oxide of $Sr_2Nb_2O_7$ and $Sr_2Ta_2O_7$ (Fig. 4), respectively. For comparison, oxides of the composition $A_2B_2O_7$ (A = Ca, Sr, B = Ta, Nb) were also prepared by the classical ceramic method. In the case of Ba-based compounds, the X-ray diffraction patterns reveal two phases, namely $Ba_5B_4O_{15}$ ($n = 5$ member of the perovskite slab series $A_nB_{n-1}O_{3n}$) and BaB_2O_6. These oxides have been reported during phase equilibrium studies of the $BaO–Nb_2O_5$ system [26]. The X-ray patterns of the calcined precursors from the soft-chemistry

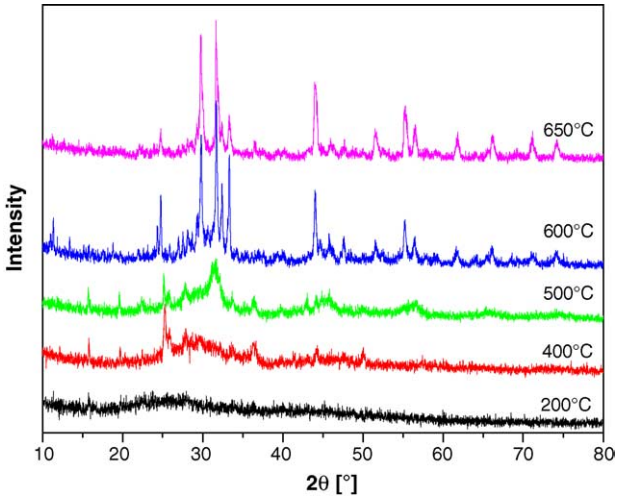

Fig. 3. X-ray profiles showing the crystallisation of the amorphous precursors at different temperatures during the synthesis process of strontium niobium oxide.

route and of the samples obtained by conventional solid state synthesis methods were found to be identical.

3.2. Ammonolysis reaction

The various oxide precursors were heated in an ammonia flow of 50–150 ml/min to synthesise the oxynitrides. For the crystalline oxides prepared by ceramic reactions, the formation of oxynitrides according to Eq. (1) was in most cases achieved at a temperature of 950 °C. Only for some of the tantalates the reaction temperature had to be increased. While $CaTaO_2N$ was formed from $Ca_2Ta_2O_7$ after 36 h at 950 °C, the temperature for ammonolysis had to be raised to 1000 °C for $SrTaO_2N$ and $BaTaO_2N$. In addition, the reaction time had to be strongly increased. Single-phase $SrTaO_2N$ was formed after 90 h, while $BaTaO_2N$ was achieved after 126 h. A similar effect was observed for the niobates: $SrNbO_2N$ was formed from $Sr_2Nb_2O_7$ in 54 h at 950 °C and $BaNbO_2N$ was

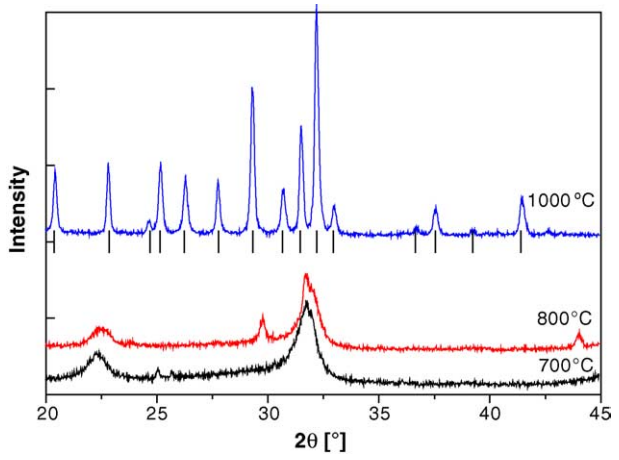

Fig. 4. Formation of crystalline $Sr_2Ta_2O_7$ from the amorphous soft-chemistry precursor.

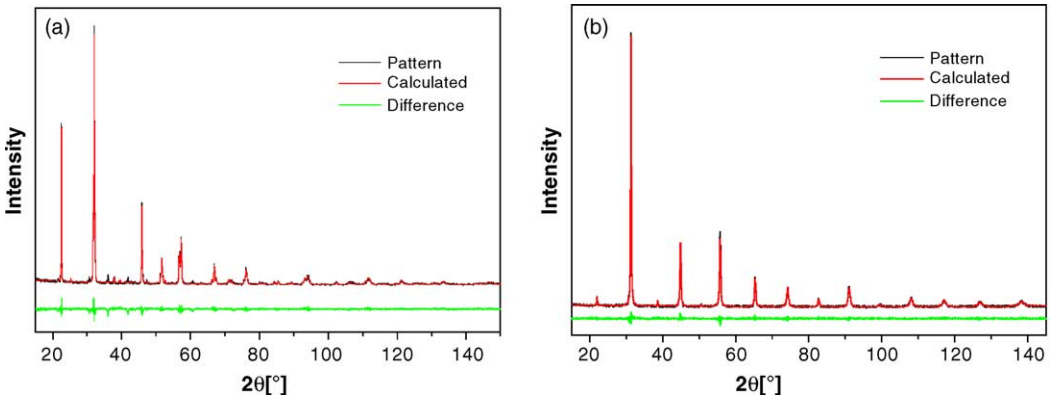

Fig. 5. Structural refinements of oxynitrides: (a) $CaNbO_2N$ and (b) $SrNbO_2N$.

formed after 90 h. The synthesis temperature for $CaNbO_2N$ is critical because NbO_xN_y is very stable at such high temperatures and cannot be eliminated. Kim et al. [21] therefore synthesised $CaNbO_2N$ with the aid of mineralisers. Mineralisers help to overcome the diffusion barrier between the ions and thus allow reactions at lower temperatures. To avoid the formation of niobium oxynitride, we prepared $CaNbO_2N$ at 750 °C in the presence of a mixture of KCl and NaCl. For the other oxynitrides, KCl was used as flux. The Ca- and Sr-tantalates were formed at 950 °C with an ammonia flow of 50 ml/min within 18 h and the Sr-niobate was obtained in 36 h. The Ba-compounds of tantalum and niobium could be prepared in 54 and 72 h, respectively. The obtained compounds were checked for the elimination of the halide by leaching the samples in distilled water and testing the filtrate with $AgNO_3$ solution. From the above-mentioned observations it is apparent that halide fluxes considerably reduce the time for the formation of oxynitrides.

$$A_2B_2O_7 + 2NH_3 \rightarrow 2ABO_2N + 3H_2O \quad (1)$$

Oxynitrides were also prepared from the xerogel precursors obtained by the soft-chemistry method. $CaTaO_2N$ and $SrTaO_2N$ were achieved at 950 °C within 36 and 54 h, respectively. $CaNbO_2N$ and $SrNbO_2N$ were formed from their xerogel precursors at a rather low temperature of 750 °C in 55 h, while the Ba-compounds were synthesised at 850 °C within 60 h.

Summarising these results it can be concluded that the formation of oxynitrides requires the longest reaction times and highest temperatures if crystalline oxides are used as starting materials. Adding halides significantly reduces the reaction time and temperature. Furthermore, these additives suppress the formation of binary (oxy)nitrides, which occurs at higher temperatures due to the reducing character of ammonia. The usage of amorphous oxide precursors lowers the reaction temperature even more. Additionally, a possible contamination of the oxynitrides by the alkali fluxes can be excluded, making it the most favourable preparation route.

3.3. Crystal structure and morphology

Crystal structures and cell parameters have been determined by Rietveld refinement calculations using the program Powder Cell [27]. As examples, the refinements of $CaNbO_2N$ (flux-assisted ceramic method) and $SrNbO_2N$ (citrate route) are presented in Fig. 5. The obtained results are consistent with the models based on the available literature [4,15–17,21,28]. For a given A-type cation the niobium and tantalum compounds were found to be isostructural. With decreasing size of the A cations, the same reduction of crystallographic symmetry as for oxide perovskites was observed. The Ba compounds proved to be cubic perovskites, while for the Sr oxynitrides a tetragonal distortion was observed. $SrNbO_2N$ was lately examined using powder neutron diffraction, revealing a partial order of the O/N ions on the two different anionic sites of the tetragonal distorted structure [29]. The Ca compounds adopt an orthorhombic structure known as the $GdFeO_3$-structure type (space group *Pnma*) [16,21,22]. A

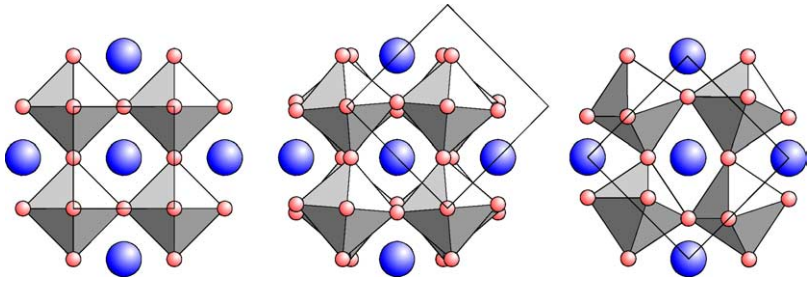

Fig. 6. Crystal structure of oxynitride perovskites: cubic [$Pm\bar{3}m$], tetragonal [$I4/mcm$], orthorhombic [*Pnma*].

Table 1
Structural and physical properties of tantalum and niobium oxynitrides

Sample	Synthesis method	Crystal system	Space group	No.	Particle size (nm)	*a* (Å)	*b* (Å)	*c* (Å)	Colour
$CaTaO_2N$	Ceramic	Orthorhombic	*Pnma*	62	200–250	5.6196	7.8879	5.5479	Yellow
$SrTaO_2N$	Ceramic	Tetragonal	*I4/mcm*	140	400–700	5.6964	–	8.0934	Orange
$BaTaO_2N$	Ceramic	Cubic	$Pm\bar{3}m$	221	200–250	4.1109	–	–	Snuff
$CaNbO_2N$	Ceramic	Orthorhombic	*Pnma*	62	400–450	5.6433	7.9068	5.5542	Ochre
$SrNbO_2N$	Ceramic	Tetragonal	*I4/mcm*	140	250–300	5.7056	–	8.1002	Snuff
$BaNbO_2N$	Ceramic	Cubic	*Pm*-3*m*	221	250–350	4.1267	–	–	Black
$CaTaO_2N$	Soft-chemistry	Orthorhombic	*Pnma*	62	350–400	5.6223	7.8940	5.5503	Yellow
$SrTaO_2N$	Soft-chemistry	Tetragonal	*I4/mcm*	140		5.6917	–	8.0777	Orange
$CaNbO_2N$	Soft-chemistry	Orthorhombic	*Pnma*	62					Ochre
$SrNbO_2N$	Soft-chemistry	Tetragonal	*I4/mcm*	140		5.7077	–	8.0985	Snuff

comparative view of the structures of the niobium perovskite oxynitrides is presented in Fig. 6. Crystallographic data and average particle sizes of the oxynitrides under investigation are given in Table 1. It is to be noted that all samples show intense colours, while their corresponding oxides are colourless. This effect can be explained considering the nature of the anionic species. Despite its higher charge, N^{3-} has a smaller electronegativity than O^{2-}. The nitride ion is therefore softer and the M–N bond exhibits a stronger covalent character than the M–O bond. This effect reduces the band gap of the compounds and leads to a shift of the optical absorption towards the visible region of the spectrum [2,25].

The morphology of the various oxynitrides and oxide materials was investigated by scanning electron microscopy. Fig. 7 shows a comparison of selected alkaline earth oxynitrides of tantalum and niobium prepared by (mineraliser-assisted) ceramic and soft-chemistry method. For the samples prepared by the conventional ceramic method, $CaTaO_2N$ consists of agglomerated irregular particles of approximately 0.2 μm diameter, whereas $SrTaO_2N$ exhibits a plate-like morphology with particles up to 1 μm size. A dense packing of very small spherical particles (<0.1 μm) was observed for $BaTaO_2N$. An illustrative example for the influence of the halide mineralisers is shown in Fig. 7d. $CaNbO_2N$ synthesised by the mineraliser-assisted ceramic method consists of highly crystalline particles with well-defined rectangular shapes and smooth surfaces. The particle sizes range from 200 to 400 nm. In contrast, $CaNbO_2N$ and $SrNbO_2N$ prepared by the soft-chemistry method appear rather foamy with highly agglomerated irregular particles ranging from a submicrometer size ($SrNbO_2N$) to l–2 μm ($CaNbO_2N$) as can be seen in Figs. 7e and f. In conclusion it can be said that the type of the A cations only slightly influences the size and shape of the product particles but a much stronger effect is achieved by changing the synthesis technique.

3.4. Thermal stability

To study the stability of the oxynitrides, annealing experiments in air were carried out. Samples were heated in a box furnace to 1000 °C with a rate of 3 °C/min. Small aliquots were taken out of the furnace at regular intervals and investi-

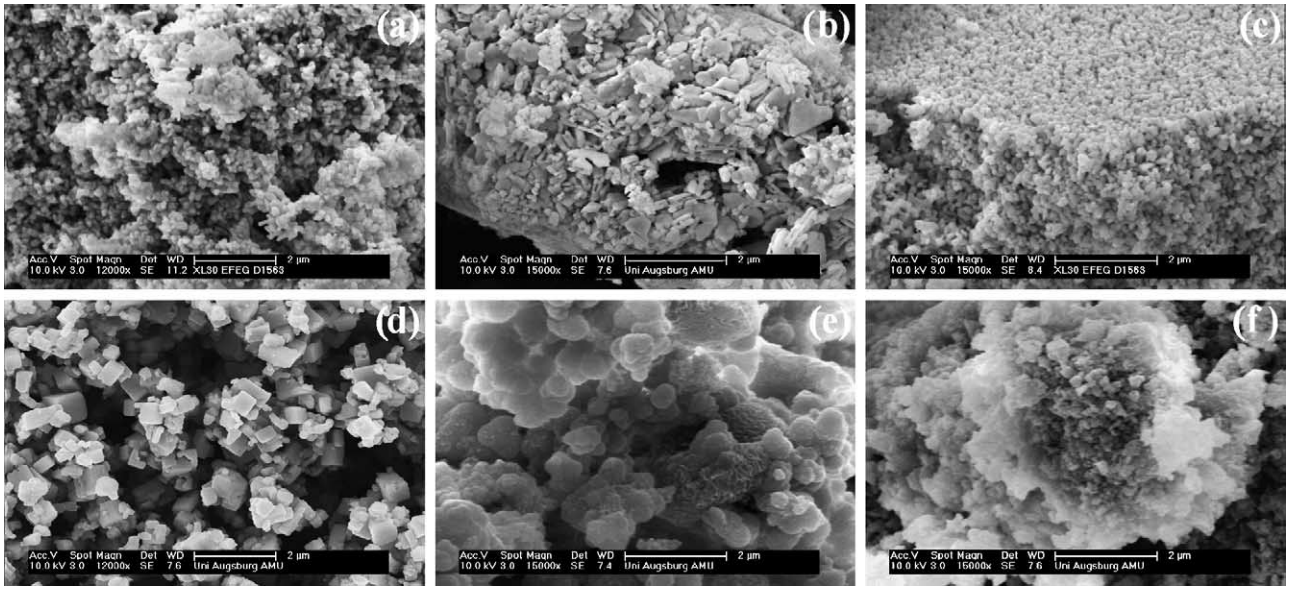

Fig. 7. . SEM images of oxynitrides: (a) $CaTaO_2N$ – ceramic method, (b) $SrTaO_2N$ – ceramic method, (c) $BaTaO_2N$ – ceramic method, (d) $CaNbO_2N$ – ceramic method + mineraliser, (e) $CaNbO_2N$ – soft-chemistry method, and (f) $SrNbO_2N$ – soft-chemistry method.

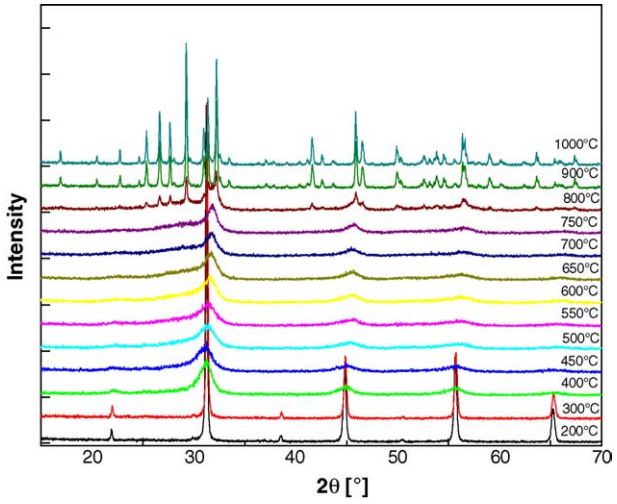

Fig. 8. XRD patterns of strontium niobium oxynitride after annealing in air at different temperatures.

gated by ex-situ XRD and Raman spectroscopy. For comparison, series of in-situ Raman spectra of selected oxynitride samples were taken in the temperature range between 20 and 600 °C in air with the samples mounted on a special heater. The ex-situ Raman spectra (recorded at room temperature on samples which were heated up to a temperature *T* and cooled down again) agree well with the corresponding in-situ Raman spectra obtained for the samples at *T*. This finding demonstrates the stability of the intermediate compounds in the thermal conversion process from the oxynitrides to the corresponding oxides and justifies our approach of comparing results obtained in situ by thermogravimetric analysis with results obtained ex situ by Raman spectroscopy and by powder XRD.

Powder X-ray diffraction revealed that at temperatures of 450–500 °C the crystallinity of the samples successively decreased resulting in broad diffraction peaks, which still resembled the basic perovskite structure. The decreasing reflection intensities reveal a nearly amorphous state. With further increase in temperature, well-resolved reflexes corresponding to the respective oxides emerge. For the different samples these peaks evolve between 800 and 1000 °C. As an example, Fig. 8 shows the X-ray patterns for the annealing of $SrNbO_2N$.

The corresponding ex-situ Raman spectra are depicted in Fig. 9. Two interesting frequency regions can be distinguished. In the lower frequency range between 100 and 1300 cm^{-1}, the evolution of a strong mode at approximately 840 cm^{-1} was observed for a temperature above 450 °C. This band can be ascribed to the NbO_6-octahedra "breathing" mode. In the high frequency region a characteristic vibrational band at 2320–2340 cm^{-1} appears. This frequency is characteristic for the stretching mode of N_2 and thus indicates the presence of dinitrogen in the material. Similar observations were made by Clarke et al. for Zr_2ON_2 [30] and Le Gendre during the oxidation of $LaTiO_2N$ [31]. This result was interpreted as a retention of N_2 molecules due to a weak interaction with the transition metal. It is to be noted that the BO_6 breathing mode and the N_2 peak first appear at the same temperature of approximately 450 °C. This indicates that the sample is completely oxidised (i.e. the oxygen stoichiometry $O_{3.5}$ is reached), while the nitrogen is retained in the crystal framework, which according to the XRD pattern, is basically still a perovskite. Apart from small differences in temperature, we found identical behaviours for all samples investigated. Marchand et al. reported similar results for compounds belonging to the perovskite type with orthorhombic distortion, K_2NiF_4 type and tetrahedral wurtzite type structures [31,32]. It therefore seems that the oxidation of the nitride ions and the retention of the formed N_2 in the crystal framework is characteristic for various kinds of oxynitrides/nitrides. Fig. 10 depicts the temperature-dependent evolution of the peak areas of the N_2-related Raman signal determined by fitting with a Voigt-type line shape (convo-

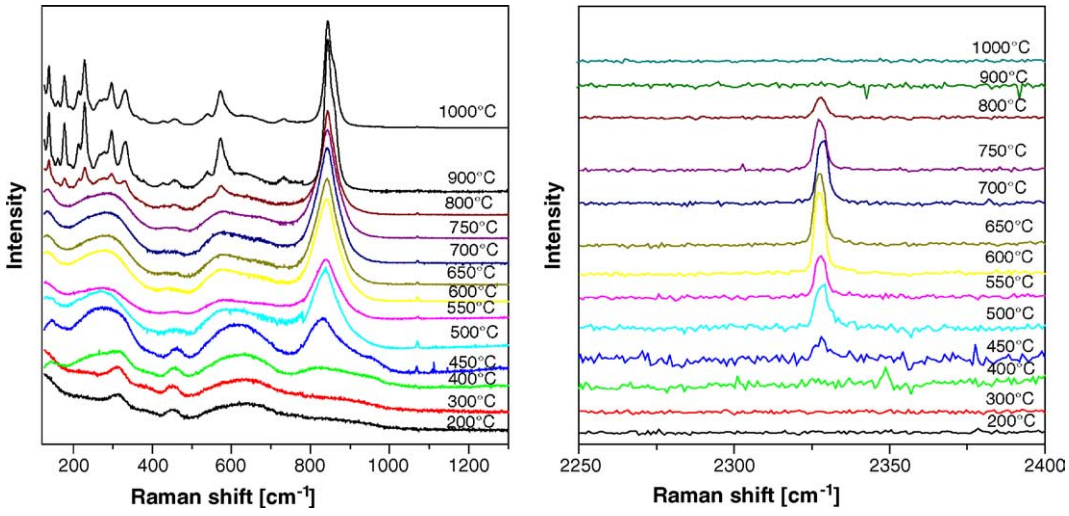

Fig. 9. Raman analysis of $SrNbO_2N$ after annealing in air at different temperatures.

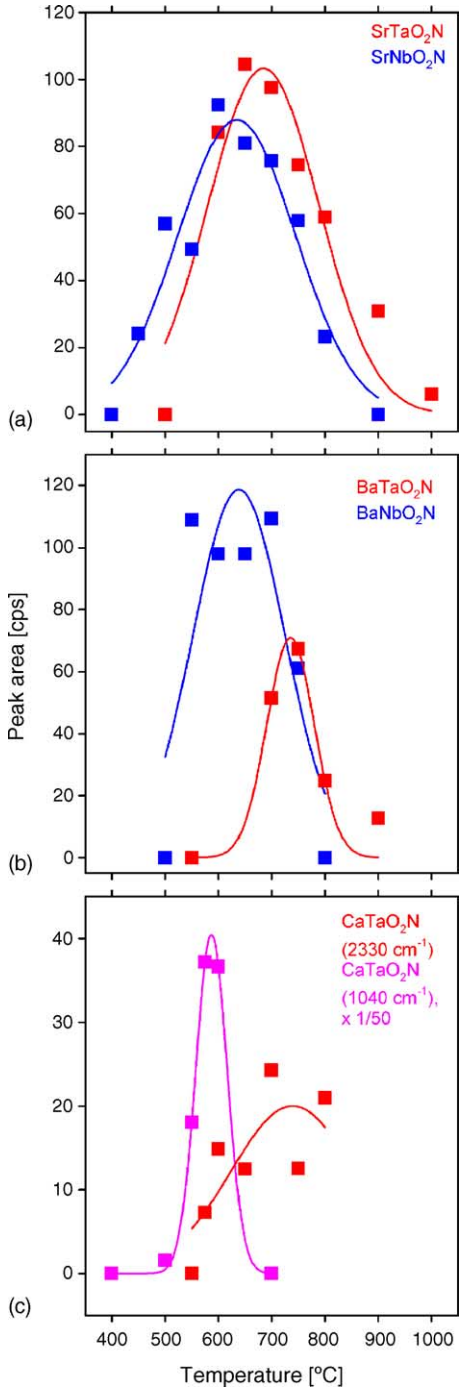

Fig. 10. Plots of the Raman intensities of the N≡N signal at 2330 cm^{-1} as a function of annealing temperature for (a) $SrNbO_2N$ and $SrTaO_2N$, (b) $BaNbO_2N$ and $BaTaO_2N$, and (c) $CaTaO_2N$. In (c) the Raman intensity of the N≡Ta signal at 1040 cm^{-1} vs. annealing temperature is also plotted.

lution of a Lorentzian line with Gaussian broadening). The spreading of the data points mainly arises because the scattering geometries vary for the different powder samples. Therefore, Gaussian fits to the data are given in the same figure as guides to the eye. It is clearly seen that the Nb-oxynitrides show the maximum intensity of the N_2 feature – and therefore presumably the highest N_2 concentration – at a lower temperature than the corresponding Ta-oxynitrides. Moreover, $CaTaO_2N$ (Fig. 11) and $SrTaO_2N$ (spectra not shown here) exhibit another characteristic Raman feature at around 1040 cm^{-1} evolving from 500 °C on and disappearing between 600 and 700 °C. For $CaTaO_2N$, in which it is rather strong, the temperature-dependent intensity of this signal is added in the lower graph of Fig. 10. It presumably originates from the vibrations of nitrogen atoms triply bound to transition metal atoms B (Ta in this case) as the observed frequency is typical of the corresponding stretch modes in several known N≡B complexes. Obviously, in both compounds there are two different complexes being responsible for the nitrogen retention as the N≡N mode at 2330 cm^{-1} is also visible in their spectra. Fig. 10 also indicates that the N≡B signal at 1040 cm^{-1} is present in a different (lower) temperature range than the N≡N signal at 2330 cm^{-1} indicating that the two features really belong to different types of complexes. The other compounds under study do not show any detectable signal in the 1040 cm^{-1} region and are thus not believed to contain complexes of the N≡B type in significant concentrations.

In addition to the ex-situ annealing experiments the thermal oxidation of the perovskite oxynitrides was studied by thermoanalytical methods under different atmospheres. Fig. 12a shows as a representative example the thermogravimetric result for the reaction of $SrNbO_2N$ in 20% O_2/80% Ar. Moreover, the mass spectra signals for different gases like N_2 ($m/e = 28$), CO_2 ($m/e = 44$) and H_2O ($m/e = 18$) are given. For a quantitative analysis of the MS data, pulses of 1 ml N_2 were added to the reaction gas at the beginning (200 °C) and at the end (1200 °C) of the thermal oxidation experiments. On analysing the TG curve we observed a characteristic increase in weight during the thermal oxidation, leading to intermediate values much higher than expected for the reaction $2SrNbO_2N + 1.5O_2 \rightarrow Sr_2Nb_2O_7 + N_2$. This weight increase started at around 425 °C and reached a maximum (mass increase = 5%) at roughly 600 °C. At higher temperatures the weight decreases almost linearly to a value of 4% at 920 °C. Above this temperature a sudden decrease of weight occurs, leading to the final oxide $Sr_2Nb_2O_7$. The intermediate weight gain apparently originates from the retention of bound dinitrogen in the fully oxidised material, as confirmed by the Raman results given above and earlier investigations [32]. The very small weight loss between 600 and 920 °C indicates that the intermediate dinitrogen-containing compound has a considerable thermal stability in a temperature range of more than 300 °C. For the different samples pronounced differences in the stability ranges of the intermediates were observed. For calcium compounds the stability of the intermediate ranged from 250 to 300 °C, for Sr compounds from 300 to 350 °C, while for Ba compounds it was in a range of 200–250 °C. By analysing the online MS signals we found that the sharp increase in weight at about 425 °C is accompanied by a partial release of nitrogen. A very small signal for CO_2 indicates the presence of traces of a carbonate phase. We assume that this peak is caused by CO_2 absorbed on the surface of the oxynitride particles. Between 610 and 920 °C

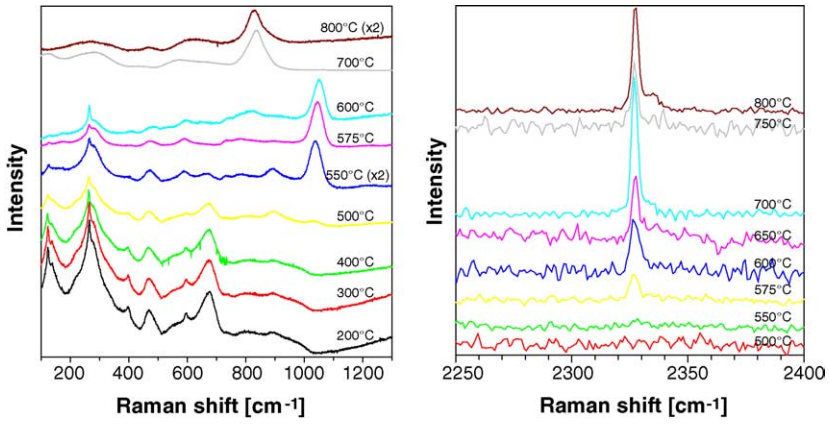

Fig. 11. Raman analysis of $CaTaO_2N$ after annealing in air at different temperatures.

the MS signal of N_2 strongly decreases, showing that the rate of N_2 evolution becomes very small. In the same temperature regime the N≡N stretching mode at approximately $\nu_{N\equiv N} = 2330\ cm^{-1}$ was observed (*vide extra*), indicating that part of the formed N_2 is retained within the lattice framework and interacts with the cations. Since the Raman wave number is very similar to the one of free nitrogen ($\nu_{N\equiv N} = 2329\ cm^{-1}$), these interactions must be rather weak. With further increase of temperature the sharp weight loss at 950 °C is again accompanied by a peak for $m/e = 28$ in the MS signal. Obviously, at this temperature the N_2 that is incorporated in the perovskite-type intermediate is released and the final oxidation product ($A_2B_2O_7$) is formed.

A dramatic change in the oxidation behaviour was observed for a lower oxygen partial pressure. Fig. 12b shows the thermal oxidation of $SrNbO_2N$ in 1% O_2. From Fig. 12b it can be seen that in this oxygen-poor atmosphere, the nitrogen is released without passing through the intermediate state of chemisorbed dinitrogen. It is to be noted that both the starting temperature of the oxidation reaction and the temperature at which the final oxide is formed are almost identical for the oxidation in 1 and 20% oxygen, respectively. Per-

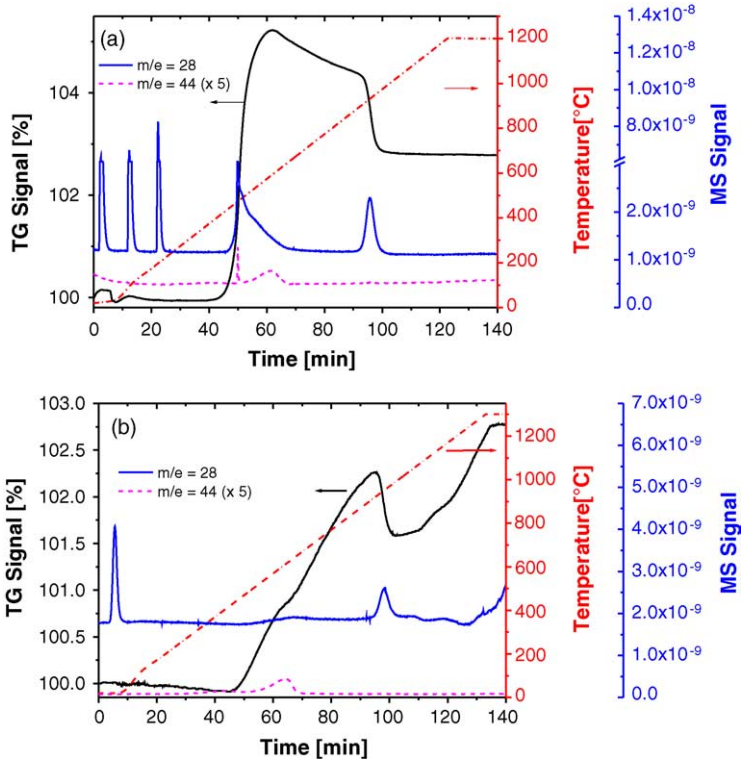

Fig. 12. TG/MS analysis of $SrNbO_2N$ in oxidising atmosphere: (a) 20% O_2 and (b) 1% O_2. Sharp peaks in the MS signal arise from external pulses of N_2, which were added to quantify the results.

haps even more interesting is the weight loss found at about 940 °C for the oxidation in 1% oxygen. From the MS signal it was found that this weight loss is also accompanied by the release of N_2. Before the final oxide ($Sr_2Nb_2O_7$) is obtained at 1010 °C, a highly anion-deficient intermediate seems to exist. The nature of this intermediate is to date completely unknown and will be the subject of further studies in the near future.

4. Conclusions

The preparation of perovskite-related oxynitrides with the general composition ABO_2N (A = Ca, Sr, Ba; Ba = Nb, Ta) was realised using different approaches including the classical solid state approach and flux-assisted reactions. Additionally, a standard soft-chemistry synthesis method using citrate complexes was developed. With the latter a significant reduction of the ammonolysis temperature was achieved. For example, $SrNbO_2N$ was formed at a 200 °C lower reaction temperature. The oxynitrides prepared by these methods adopt very different particle sizes and shapes. The crystal structure and phase purity was verified using XRD Rietveld refinements. The thermal oxidation to the corresponding oxides revealed an unusual weight gain in an atmosphere containing 20% oxygen. On the basis of thermogravimetric measurements, mass spectroscopy of the volatile reaction products, X-ray diffraction and Raman spectroscopy, intermediate N_2-containing compounds were identified for all oxynitrides studied. The intermediate phases of $CaTaO_2N$ and $SrTaO_2N$ show the presence of additional N≡B (B = transition metal) complexes. These intermediates exhibited a considerable thermal stability and resembled the basic perovskite framework with a very low crystallinity. When the oxidation was carried out in 1% O_2, the temperature for the beginning and completion of the oxidation remained unchanged, but no intermediate transition stage due to N_2 retention was observed. This reaction apparently involved a highly anion-deficient compound the nature of which requires further investigations.

Acknowledgements

The authors greatly acknowledge the Deutsche Forschungsgemeinschaft (SPP 1136) for financial support. We thank Dr. F. Weller and Prof. W. Massa from the Department of Chemistry of the Philipps-University of Marburg for their help with the in-situ Raman measurements.

References

[1] R.H. Mitchell, Perovskites – Modern and Ancient, 1st ed., Almaz Press, Inc., Ontario, 2002.
[2] R. Marchand, Y. Laurent, J. Guyader, P.L. Haridon, P. Verdier, J. Eur. Ceram. Soc. 8 (1991) 197–213.
[3] R. Asahi, T. Morikawa, T. Ohwaki, K. Aoki, Y. Taga, Science 293 (2001) 269–271.
[4] X. Gouin, R. Marchand, Y. Laurent, F. Gervais, Solid State Commun. 93 (1995) 857–859.
[5] P. Antoine, R. Assabaa, P.L. Haridon, R. Marchand, Y. Laurent, C. Michel, B. Raveau, Mater. Sci. Eng. B 5 (1989) 43–46.
[6] E. Günther, M. Jansen, Mater. Res. Bull. 36 (2001) 1399–1405.
[7] S. Esmaeilzadeh, J. Grins, T. Hörlin, Mater. Sci. Forum 325/326 (2000) 11–16.
[8] R. Brayner, G. Djega-Mariadassou, G. Marques da Cruz, J.A.J. Rodrigues, Catal. Today 57 (2000) 225–229.
[9] A. Kasahara, K. Nukumizu, G. Hitoki, T. Takata, J.N. Kondo, M. Hara, H. Kobayashi, K. Domen, J. Phys. Chem. A 106 (2002) 6750–6753.
[10] M. Bose, D.N. Bose, D.K. Basa, Mater. Lett. 52 (2002) 417–422.
[11] M. Modreanu, N. Tomozeiu, P. Cosmin, M. Gartner, Thin Solid Films 337 (1999) 82–84.
[12] M. Jansen, H.P. Letschert, Nature 404 (2000) 980–982.
[13] H. Bert, Glas en keramiek 21 (2000) 23.
[14] I.D. Fawcett, K.V. Ramanujachary, M. Greenblatt, Mater. Res. Bull. 32 (1997) 1565–1570.
[15] R. Marchand, F. Pors, Y. Laurent, Rev. Int. Hautes Tempér. Réfract., Fr. 23 (1986) 11–15.
[16] E. Günther, R. Hagenmayer, M. Jansen, Z. Anorg, Allg. Chem. 626 (2000) 1519–1525.
[17] S.J. Clarke, K.A. Hardstone, C.W. Michie, M.J. Rosseinsky, Chem. Mater. 14 (2002) 2664–2669.
[18] I. Elphinstone, A. Hendry, Br. Ceram. Proc. 45 (1989) 15–22.
[19] R. Schlichenmaier, E. Schweda, J. Strähle, T. Vogt, Z. Anorg. Allg. Chem. 619 (1993) 367–373.
[20] N. Arumugam, A. Hönnerscheid, M. Jansen, Z. Anorg. Allg. Chem. 629 (2003) 939–941.
[21] Y.-I. Kim, P.M. Woodward, K.Z. Baba-Kishi, C.W. Tai, Chem. Mater. 16 (2004) 1267–1276.
[22] J. Rooke, M. Weller, Solid State Phenom. 90/91 (2003) 417–422.
[23] S.J. Clarke, B.P. Guinot, C.W. Michie, M.J.C. Calmont, M.J. Rosseinsky, Chem. Mater. 14 (2002) 288–294.
[24] M. Popa, M. Kakihana, Catal. Today 78 (2003) 519–527.
[25] F. Tessier, R. Marchand, J. Solid State Chem. 171 (2003) 143–151.
[26] T.A. Vanderah, T.R. Collins, W. Wong-Ng, R.S. Roth, L. Farber, J. Alloys Compd. 346 (2002) 116–128.
[27] W. Kraus, G. Nolze, J. Appl. Cryst. 29 (1996) 301–303.
[28] F. Pors, P. Bacher, R. Marchand, Y. Laurent, G. Roult, Rev. Int. Hautes Temper. Réfract., Fr. 24 (1988) 239–246.
[29] S.G. Ebbinghaus, A. Weidenkaff, A. Rachel, A. Reller, Acta Cryst. C 60 (2004) 191–193.
[30] S.J. Clarke, C.W. Michie, M.J. Rosseinsky, J. Solid State Chem. 146 (1999) 399–405.
[31] L. Le Gendre, R. Marchand, B. Piriou, Eur. J. Solid State Inorg. Chem. 34 (1997) 973–982.
[32] L. Le Gendre, R. Marchand, Y. Laurent, J. Eur. Ceram. Soc. 17 (1997) 1813–1818.